

# Effects of Glatiramer Acetate and Interferon- $\beta$ on Neurodegeneration in a Model of Multiple Sclerosis

## A Comparative Study

Katharina Maier,\* Antje V. Kuhnert,\*  
Naimeh Taheri,\* Muriel B. Sättler,\*  
Maria K. Storch,<sup>†</sup> Sarah K. Williams,\*  
Mathias Bähr,\* and Ricarda Diem\*

From the Neurologische Universitätsklinik,\* Göttingen, Germany;  
and the Neurologische Universitätsklinik,<sup>†</sup> Graz, Austria

**Axonal destruction and neuronal loss occur early during multiple sclerosis (MS), an autoimmune inflammatory central nervous system disease that frequently manifests with acute optic neuritis. Glatiramer acetate (GA) and interferon- $\beta$ -1b (IFN- $\beta$ -1b) are two immunomodulatory agents that have been shown to decrease the frequency of MS relapses. However, the question of whether these substances can slow neurodegeneration in MS patients is the subject of controversy. In a rat model of experimental autoimmune encephalomyelitis, we investigated the effects of GA and IFN- $\beta$ -1b on the survival of retinal ganglion cells (RGCs), the neurons that form the axons of the optic nerve. For each substance, therapy was started 14 days before immunization, on the day of immunization, or on the day of clinical disease onset. After myelin oligodendrocyte glycoprotein-induced experimental autoimmune encephalomyelitis became clinically manifest, optic neuritis was monitored by recording visual evoked potentials. The function of RGCs was measured by electroretinograms. Although early GA or IFN- $\beta$ -1b treatment showed benefit on disease activity, only treatment with GA exerted protective effects on RGCs, as revealed by measuring neurodegeneration and neuronal function. Furthermore, we demonstrate that this GA-induced neuroprotection does not exclusively depend on the reduction of inflammatory infiltrates within the optic nerve. (*Am J Pathol* 2006, 169:1353–1364; DOI: 10.2353/ajpath.2006.060159)**

Multiple sclerosis (MS) is a chronic inflammatory demyelinating disease of the central nervous system (CNS). Besides demyelination and inflammation, pathology of MS is associated with destruction of axons and consecutive neuronal cell death that leads to progressive clinical disability in patients.<sup>1,2</sup> Interferon- $\beta$  (IFN- $\beta$ ) and glatiramer acetate (GA) represent two immunomodulatory agents that have shown clinical benefits in large trials of relapsing-remitting MS.<sup>3–5</sup> However, the question of whether these substances have any influence on neurodegenerative aspects in MS patients causes contentious discussion.<sup>6–8</sup> The results of recent studies suggest complex, different mechanisms of action on humoral and T-cellular immune responses.<sup>9</sup> In addition to their immunomodulatory properties, neurobiological effects have been described for both of these substances. Whereas GA has been shown to stimulate secretion of brain-derived neurotrophic factor (BDNF) by GA-sensitive lymphocytes,<sup>10</sup> IFN- $\beta$  promotes production of nerve growth factor by endothelial cells.<sup>11</sup> The consequences of these findings for neuronal survival and electrophysiological function of neurons have not been clarified so far.

In the present study, we used myelin oligodendrocyte glycoprotein (MOG)-induced experimental autoimmune encephalomyelitis (EAE), a model that produces a wide range of pathological lesions similar to MS.<sup>12–15</sup> Whereas the amount of spinal cord lesions in this model shows a certain variability, 90% of female brown Norway (BN) rats develop acute optic neuritis within 3 weeks of immunization with MOG.<sup>14</sup> In a previous study, we have shown that the inflammatory attack against myelin components and optic nerve axons in MOG-EAE leads to acute apoptotic death of retinal ganglion cells (RGCs).<sup>16</sup> We also ob-

Supported by the Medical Faculty of the University of Göttingen (junior research group, to R.D.), Schering AG Deutschland, TEVA Pharmaceuticals Israel, and the Gemeinnützige Hertie-Stiftung.

Accepted for publication June 20, 2006.

Address reprint requests to Katharina Maier, Neurologische Universitätsklinik, Robert-Koch-Str. 40, D-37075 Göttingen, Germany. E-mail: kmaier@gwdg.de.

served a reduction in the density of RGCs, axons of which form the optic nerve, during the preclinical period of MOG-EAE.<sup>17</sup>

IFN- $\beta$ -1b or GA in our present study was given according to three different treatment regimens: either starting at the day of disease onset to reflect the clinical situation or beginning 14 days before and at the day of immunization as a prophylactic treatment. Under these treatments, we investigated incidence and severity of optic neuritis. Further, we assessed survival and function of RGCs as well as that of their axons. The function of the optic system was tested by recording visual evoked potentials (VEPs) and electroretinograms (ERGs) in response to flash and pattern stimuli. In addition, we compared the influence of IFN- $\beta$ -1b and GA on intraneuronal apoptosis- or survival-related signaling cascades.

## Materials and Methods

### Rats

Female BN rats of 8 to 10 weeks of age were used in all experiments. They were obtained from Charles River (Sulzfeld, Germany) and kept under environmentally controlled conditions. All experiments were performed in compliance with the relevant laws and institutional guidelines. These experiments have been approved by the local authorities of Braunschweig, Germany.

### Induction and Evaluation of EAE

The rats were anesthetized by inhalation of diethyl ether and were then injected intradermally at the base of the tail with a total volume of 100  $\mu$ l of inoculum, containing 50  $\mu$ g of MOG (kindly provided by C. Stadelmann and D. Merkler, Department of Neuropathology, Neurologische Universitätsklinik, Göttingen, Germany) in saline emulsified (1:1) with complete Freund's adjuvant (Sigma, St. Louis, MO) containing 200  $\mu$ g of heat-inactivated *Mycobacterium tuberculosis* (strain H 37 RA from Difco Laboratories, Detroit, MI). Rats were scored for clinical signs of EAE and weighed daily. This score reflects the amount of spinal cord lesions and does not include visual symptoms or correlate with the severity of optic neuritis.<sup>14,18</sup> The signs were scored as follows: grade 0.5, distal paresis of the tail; grade 1, complete tail paralysis; grade 1.5, paresis of the tail and mild hind leg paresis; grade 2.0, unilateral severe hind leg paresis; grade 2.5, bilateral severe hind limb paresis; grade 3.0, complete bilateral hind limb paralysis; grade 3.5, complete bilateral hind limb paralysis and paresis of one front limb; grade 4, complete paralysis (tetraplegia), moribund state, or death. Day 1 of EAE was defined as the day when the first motor symptoms were detected.

### Retrograde Labeling of RGCs

Adult BN rats were anesthetized with 10% ketamine (0.75 ml/kg; Atarost GmbH and Co., Twistringen, Germany) together with 2% xylazine (0.35 ml/kg; Albrecht, Aulen-

dorf, Germany), the skin was incised mediosagittally, and holes were drilled into the skull above each superior colliculus (6.8 mm dorsal and 2 mm lateral from bregma). Two  $\mu$ l of the fluorescent dye Fluorogold (FG, 5% in normal saline; Fluorochrome Inc., Englewood, CO) were injected stereotactically into both superior colliculi.

### Treatment of Animals

Animals were randomly assigned to eight different groups containing eight animals each. The verum groups were treated with IFN- $\beta$ -1b (Betaferon; Schering, Berlin, Germany)  $3 \times 10^5$  U s.c. every 2nd day as described by van der Meide and colleagues<sup>19</sup> or with daily subcutaneous applications of GA (Copaxone; Teva Pharmaceuticals, Petach Tikva, Israel) in a dosage of 50  $\mu$ g. One group (pre) for each substance received pretreatment with IFN- $\beta$ -1b or GA started 14 days before immunization. In the early treatment groups, therapy with IFN- $\beta$ -1b or GA was started at the day of immunization. The rationale for this early treatment lies in our recent observation that significant RGC death started at day 7 after immunization, corresponding to a time point at least 1 week before clinical onset of the disease.<sup>17</sup> In an attempt to reflect the clinical situation in MS patients, the late treatment groups received IFN- $\beta$  and GA, respectively, from day 1 of MOG-EAE onwards. Each treatment was continued until day 21 of the disease. The respective control animals received 0.5 ml of 0.9% NaCl s.c. from the day of immunization onwards either as a daily application (after the treatment intervals of GA) or given every 2nd day according to the treatment protocol of IFN- $\beta$ . Pre-experiments with application of vehicle (daily or every 2nd day) throughout the different treatment periods (14 days before immunization, from immunization, or disease manifestation onwards) showed no differences concerning electrophysiological or histopathological data.

### Electrophysiological Recordings

The rats were anesthetized by intraperitoneal injection of ketamine together with xylazine as described above and mounted on a stereotaxic device. Recordings of VEPs and ERGs were performed as described earlier.<sup>16</sup> These measurements were done at clinical onset of EAE. To monitor the disease course and to investigate therapeutic effects of the different treatment regimens, measurements of VEPs and ERGs were repeated on day 8 of the disease.

### Quantification of RGC Density

At day 21 of MOG-EAE, the rats received an overdose of chloral hydrate and were perfused via the aorta with 4% paraformaldehyde in phosphate-buffered saline. The brain along with the optic nerves and both eyes were removed, and the retinas were dissected and flat-mounted on glass-slides. They were examined by fluorescence microscopy (Axiophot 2; Zeiss, Göttingen, Germany) using a UV filter (365/397 nm). RGC densities were

determined by counting labeled cells in three areas (62,500  $\mu\text{m}^2$ ) per retinal quadrant at three different eccentricities of 1/6, 3/6, and 5/6 of the retinal radius. Cell counts were performed by two independent investigators following a blind protocol. One-way analysis of variance followed by Bonferroni correction was used to analyze the RGC. A *P* value of less than 0.05 was considered to be statistically significant.

### Cell Culture

Primary RGCs were obtained from 6-day-old Wistar rats, according to a two-step immunopanning protocol described previously.<sup>20</sup> Cells were seeded into poly-D-lysine (0.01 mg/ml)-coated 96-well plates at a density of 5000 cells per well. Cultures were maintained in serum-free medium (Neurobasal; Invitrogen, Karlsruhe, Germany) containing glutamine, cysteine, B27 supplement, sodium pyruvate, triiodothyronine, and Sato's medium (transferrin, bovine serum albumin, progesterone, putrescine, and sodium selenite) supplemented with saturating concentrations of forskolin, BDNF, ciliary neurotrophic factor, and insulin at 37°C in 5% CO<sub>2</sub>. After 24 hours, medium was removed from the cells and replaced with medium containing various concentrations (10 to 300,000 U/ml) of IFN- $\beta$ -1b. Cells maintained in normal serum-free medium containing neurotrophins served as controls.

### Cell Viability Studies

Forty-eight hours after addition of IFN- $\beta$ -1b, cell viability was assessed using a (3,4,5-dimethylthiazol-2-yl)-2,5-diphenyl tetrazolium bromide (MTT) reduction assay.<sup>21</sup> MTT was added to the wells at a final concentration of 0.5 mg/ml, for 1 hour at 37°C. Viable cells with active mitochondria cleaved the tetrazolium ring into a visible blue formazan product and were visualized by bright-field microscopy. The number of surviving cells in eight fields of view in each of three wells was counted per concentration of IFN- $\beta$ -1b. Results are expressed as a percentage of controls.

### Western Blotting

Animals received an overdose of chloral hydrate, and the eyes were removed before perfusion with PFA. Eight eyes per treatment or vehicle group were included into the Western blot analysis. Retinas were homogenized, lysed (150 mmol/L NaCl, 50 mmol/L Tris, pH 8.0, 2 mmol/L ethylenediaminetetraacetic acid, 1% Triton) on ice for 20 minutes, and cell debris was pelleted at 14,000  $\times g$  for 15 minutes. The protein concentration of the supernatant was determined using the BCA reagent (Pierce, Rockford, IL). The Western blot analysis on retinal lysates was performed as described elsewhere.<sup>22</sup> After incubation with the primary antibody against BDNF (Abcam, Cambridge, UK) [1:1000 in 1% skim milk in 0.1% Tween 20 in phosphate-buffered saline (TBS-T)], membranes were washed in TBS-T and incubated with horseradish peroxidase-conjugated secondary antibodies against rabbit

IgG (1:1000 in TBS-T; Santa Cruz Biotechnology Inc., Santa Cruz, CA). Labeled proteins were detected using the ECL-plus reagent (Amersham, Arlington Heights, IL).

After incubation with the primary antibody against phospho-p44-phospho-p42 mitogen-activated protein kinases (MAPKs) (Thr202/Tyr204, 1:250 in 1% skim milk in TBS-T; New England Biolabs GmbH, Schwalbach, Germany) or against p44-p42 MAPKs (sc-93-G, 1:500 in 1% skim milk in TBS-T; Santa Cruz Biotechnology), membranes were washed in TBS-T and incubated with horseradish peroxidase-conjugated secondary antibodies against goat IgG (1:3000 in TBS-T; Santa Cruz Biotechnology).

For Western blot analysis of Bcl-2 and Bax levels, the primary antibody (sc-7382; Santa Cruz Biotechnology) was diluted 1:200 in 5% skim milk in TBS-T; for protein detection, a horseradish peroxidase-conjugated secondary antibody against mouse IgG was used (1:2000 in 1% skim milk in TBS-T; Santa Cruz Biotechnology).

After incubation with the primary antibody against phospho-Akt (1:1000 in 5% bovine serum albumin in TBS-T; New England Biolabs GmbH) or Akt (1:1000 in 1% skim milk in TBS-T; New England Biolabs GmbH), membranes were washed in TBS-T and incubated with horseradish peroxidase-conjugated secondary antibodies against rabbit IgG (1:2500 in 1% skim milk; Santa Cruz Biotechnology). For Western blot analysis of  $\beta$ -tubulin as a housekeeping protein, the primary antibody (Sigma-Aldrich, Munich, Germany) was diluted 1:1000 in TBS-T. Secondary antibody against mouse IgG (1:2000 in 5% skimmed milk; Santa Cruz Biotechnology) was applied.

### Histopathology

Histological evaluation was performed on paraformaldehyde-fixed, paraffin-embedded sections of optic nerves at day 21 of MOG-EAE. Sections were stained with Luxol-fast blue and Bielschowsky's silver impregnation to assess demyelination and axonal pathology, respectively, as previously described.<sup>14</sup> The determination of axonal densities and demyelinated areas was also described earlier.<sup>18</sup> The two independent investigators who performed neuropathological examinations were blinded to the electrophysiological results of the study as well as to the applied treatment regimen. Statistical significance was assessed using one-way analysis of variance followed by Duncan's test.

In addition, we performed staining for amyloid precursor protein (APP) (Boehringer, Mannheim, Germany), CD45 (BD Biosciences, Franklin Lakes, NJ), CD3, and ED1 as well as hematoxylin and eosin (H&E) staining (Serotec, Düsseldorf, Germany) on paraffin-embedded sections of the optic nerve. CD3, CD45, ED1, and H&E immunohistochemistry was used to quantify the extent of inflammation. For CD3 and CD45 staining, marked cells were counted at 1000-fold magnification in 12 standardized microscopic fields of 2500  $\mu\text{m}^2$ . For ED1 and H&E staining, the degree of inflammation was evaluated using the following histological score: grade 0, no inflammatory infiltration; grade 1, subarachnoid cell infiltration; grade

2, diffuse subarachnoidal and foci of parenchymal infiltration; grade 3, diffuse and widespread parenchymal infiltration.

## Results

### Clinical Disease Course

In the GA pretreatment group, the incidence of manifest EAE was suppressed: only three of eight animals developed signs related to an affection of the motor system. In contrast, the incidence of optic neuritis in this animal group, as revealed by electrophysiological assessment, reached 100%. In both pretreatment groups, the onset of EAE was significantly delayed to day 21 after immunization when compared with the respective vehicle-treated control groups (day  $20.7 \pm 2.6$  under GA treatment versus  $13.3 \pm 1.5$  for vehicle; day  $22.1 \pm 3.2$  in IFN- $\beta$ -1b-treated animals versus  $12.8 \pm 1.1$  under vehicle treatment; mean  $\pm$  SEM;  $P < 0.05$ ) (Figure 1). Treatment with IFN- $\beta$ -1b, started at the day of immunization (early treatment), also led to a significantly later onset of disease (day  $19.1 \pm 1.4$  after immunization versus day  $12.8 \pm 1.1$  in vehicle-treated animals;  $P < 0.05$ ) (Figure 1). In contrast, the disease onset in the rat group that received GA from the day of immunization onwards did not differ from that of both late treatment and vehicle-treated groups, respectively, as shown in Figure 1. Despite the delay in disease manifestation in the pretreatment and early treatment groups of IFN- $\beta$ -1b, the mean clinical scores at days 1 and 8 of MOG-EAE in these animals were similar when compared with those of the respective control group (Figure 1). The mean clinical score in the GA pretreatment group was significantly lower in comparison to vehicle-treated animals at day 8 of the disease ( $1.2 \pm 0.1$  under GA pretreatment and  $3 \pm 0.1$  for vehicle; mean  $\pm$  SEM;  $P < 0.05$ ) (Figure 1). However, the clinical outcome at the end of the study (day 21 of MOG-EAE) showed no significant differences between IFN- $\beta$ -1b-, GA-, and vehicle-treated rats after the different treatment regimens (Figure 1).

### Assessment of Visual Functions

To diagnose optic neuritis *in vivo* and to examine the electrophysiological function of RGCs, we performed VEP and ERG recordings in response to flash and pattern stimulation. Each eye was assessed separately. With VEP flash stimulation, we tested the axonal signaling of the optic nerve. A potential in response to flash light corresponds to the ability of an animal to discriminate between light or dark. Pattern VEP recordings were performed to estimate the animal's visual acuity. ERG measurements in response to flash stimulation indicate an intact function of the whole retina, whereas ERG potentials induced by pattern stimulation are a specific electrophysiological marker for RGCs. Recently, we have shown that healthy sham-immunized rats have visual acuity values of  $1.31 \pm 0.16$  cyc/degree determined by pattern VEP recordings and  $1.10 \pm 0.13$  cyc/degree in the pattern ERG measure-

ments.<sup>16</sup> Further, we have excluded concomitant uveoretinitis, which could influence the electrophysiological measurements in our model, by immunohistochemistry against T-cell receptors as well as against lysosomal membrane-related antigens on macrophages and microglia.<sup>16</sup> The electrophysiological results of the different treatment groups in our present study are summarized in Tables 1 and 2. Comparing all treatment protocols, only pretreatment with GA and, to a lesser extent, early GA therapy led to partial improvement of VEP responses to pattern stimulation and thereby to a detectable visual acuity at day 1 and/or day 8 of MOG-EAE (Table 1). In contrast, in all three IFN- $\beta$ -1b-treated groups, the reduction of visual acuity was similar to that observed in vehicle-treated animals (Table 2).

In the flash ERG measurements, most of the animals (53 of 64 measured eyes) showed intact function of the whole retina at the day of disease onset as indicated by ERG responses to flash stimulation (Table 1). With respect to this electrophysiological parameter, five animals were discordant as ERG responses to flash light were produced by only one eye. Recordings of ERGs in response to pattern stimulation revealed no differences between IFN- $\beta$ -1b- and vehicle-treated animals. In GA-treated rats in contrast, ERG results after pattern stimulation at days 1 and 8 of MOG-EAE were better than controls if GA was given as a pretreatment (Figure 2). The ERG responses to pattern stimulation in the GA early treatment group showed better results at day 1 of MOG-EAE and a trend toward a better outcome at day 8 of the disease (Table 1).

### Retinal Ganglion Cell Counts

To compare the functional data from RGCs obtained by pattern ERG measurements with their survival rates, we counted FG-positive cells at day 21 of MOG-EAE in the different treatment groups. Recently, we demonstrated that significant apoptotic cell death of RGC occurs during MOG-induced optic neuritis. In control retinas of healthy complete Freund's adjuvant-immunized rats, mean RGC density was  $2730 \pm 145$  cells/mm<sup>2</sup>.<sup>23</sup> Pretreatment with GA for 14 days in our present study resulted in RGC counts of  $1756 \pm 131.1$  per mm<sup>2</sup> (mean  $\pm$  SEM,  $P < 0.0001$  when compared with vehicle; Figure 3, A, D, and E). The animals that received GA from the day of immunization onwards also showed a significantly increased RGC survival at day 21 of MOG-EAE ( $1052 \pm 61.6$  RGCs/mm<sup>2</sup>,  $P < 0.0001$  when compared with vehicle) (Figure 3, B, D, and E). However, GA treatment started at the day of the occurrence of the first clinical signs did not improve the number of surviving RGCs when compared with vehicle-treated controls ( $444.4 \pm 46.6$  RGCs/mm<sup>2</sup> versus  $468.8 \pm 54.3$  for vehicle; Figure 3, C, D, and E). In contrast to the corresponding treatment protocol of GA, pretreatment with IFN- $\beta$ -1b started 14 days before immunization did not exert any rescue effect on RGCs ( $743.8 \pm 51.6$  RGCs/mm<sup>2</sup> versus  $599.8 \pm 36.4$  in vehicle-treated animals; mean  $\pm$  SEM) (Figure 4, A–C). Early and late treatment with IFN- $\beta$ -1b did not result in increased RGC

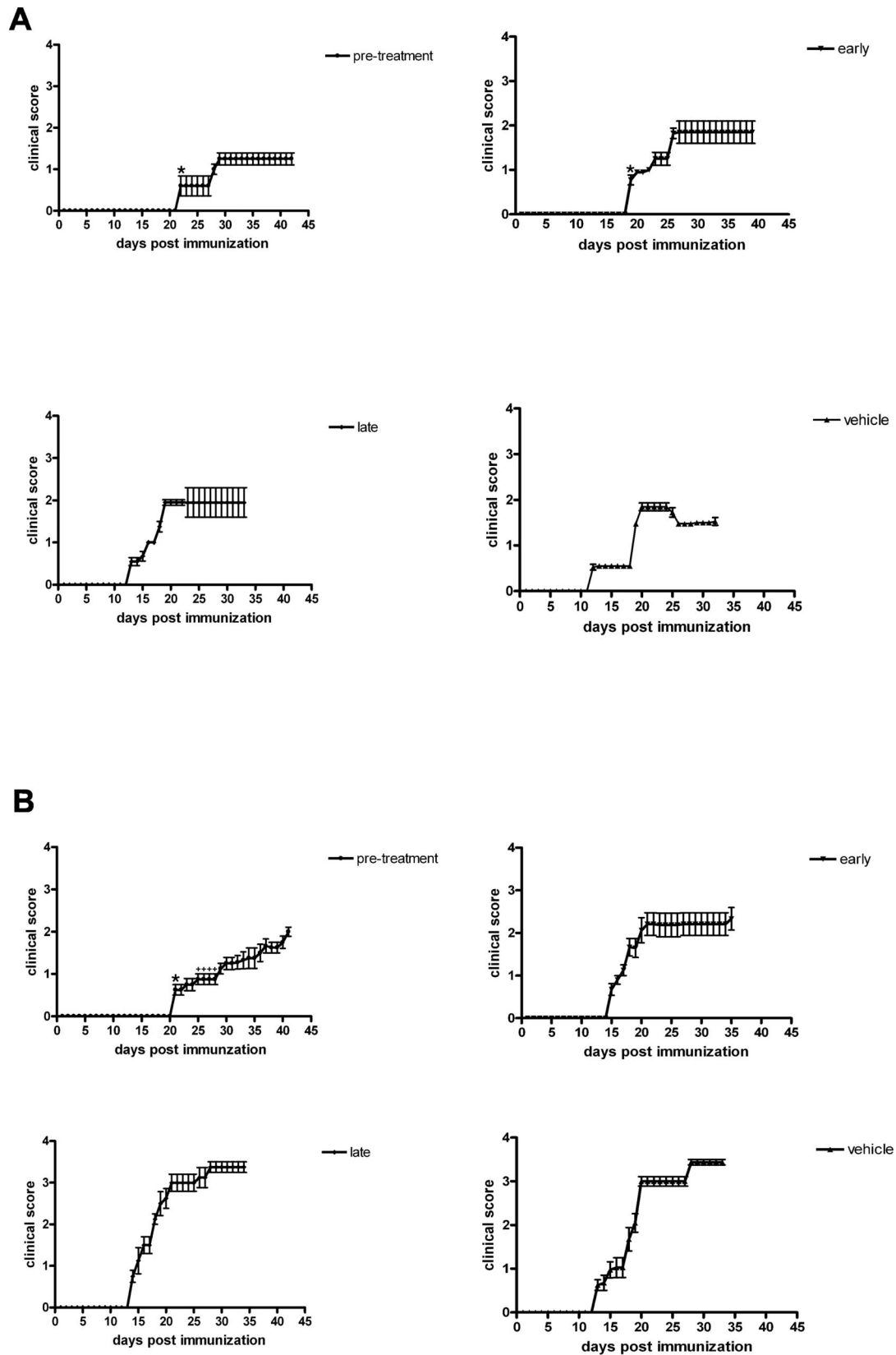


**Figure 1.** Clinical score of IFN- $\beta$ -1b (A) and GA-treated rats (B) after the different treatment regimes (pretreatment, early treatment, late treatment, vehicle-treated control group). Each value represents mean  $\pm$  SEM of the daily neurological score. Only rats with motor symptoms were included in this figure and for the statistical analysis of the general neurological score. In the GA pretreatment group only three of eight animals developed motor symptoms (in contrast to optic neuritis that was detected in eight of eight animals in that group). In all other rat groups, incidence of motor symptoms reached 100%. \*Statistically significant delay in disease onset (one-way analysis of variance followed by Duncan's test;  $P < 0.05$ ). +Statistically significant lower disease score when compared with the respective control group.

**Table 1.** Results of Visual Evoked Potentials (VEPs) and Electroretinograms (ERGs) Obtained on Days 1 and 8 of MOG-EAE (EAEd1 or EAEd8) in GA-Treated Animals and the Corresponding Control Group

	VEP EAEd1 flash	VEP EAEd8 flash	VEP EAEd1 pattern	VEP EAEd8 pattern	ERG EAEd1 flash	ERG EAEd8 flash	ERG EAEd1 pattern	ERG EAEd8 pattern
Pretreatment	6/8	8/8	0.56 ± 0.12 cyc/°*	0.38 ± 0.06 cyc/°*	8/8	8/8	0.51 ± 0.1 cyc/°*	0.42 ± 0.08 cyc/°*
Early therapy	6/8	2/8	0.26 ± 0.06 cyc/°*	0.13 cyc/°	8/8	7/8	0.3 ± 0.04 cyc/°*	0.16 ± 0.01 cyc/°
Late therapy	3/8	1/8	—	—	8/8	6/8	—	—
Vehicle	3/8	1/8	—	—	6/8	6/8	—	—
Control: CFA- immunized (day 18 p.i.)	8/8		1.31 ± 0.16 cyc/° <sup>†</sup> (day 18 p.i.)		8/8 (day 18 p.i.)		1.10 ± 0.13 cyc/° <sup>†</sup> (day 18 p.i.)	

\*Statistically significant when compared with vehicle-treated animals ( $P < 0.05$ ).

<sup>†</sup>Statistically significant when compared with GA-treated animals ( $P < 0.05$ ).

Control rats immunized with CFA were measured on day 18 after immunization (p.i.) as described previously.<sup>16</sup> The number of eyes with detectable potentials to flash stimulation is given as the number of total tested eyes in each group ( $x/8$ ). The results from pattern stimulation are given as visual acuity values calculated from VEP or ERG amplitudes and the spatial frequency of the pattern stimulation. —, Indicates groups with no detectable responses to pattern stimulation or values less than 0.13 cycle/degree (cyc/°) (which is the threshold of visual acuity detectable by this method).

counts as well ( $562.6 \pm 36.3$  cells/mm<sup>2</sup> in the early and  $665.2 \pm 82.1$  cells/mm<sup>2</sup> in the late treatment group; mean ± SEM) (Figure 4C).

### Retinal Ganglion Cell Viability Studies

We investigated whether IFN-β-1b has a direct toxic effect on RGCs using immunopurified postnatal RGCs. Forty-eight hours after application of 10 to 300,000 U/ml IFN-β-1b in culture, the number of surviving RGCs was quantified by MTT assay. There was found to be no significant difference in the number of surviving RGCs after treatment with all concentrations of IFN-β-1b, in comparison to cells cultured in normal growth media (Figure 4D).

### Inflammatory Infiltration of the Optic Nerve

To investigate the severity of optic neuritis in the different treatment groups, we performed immunohistochemistry with an antibody against CD3, CD45, and ED1. In general, only a few CD3- and CD45-positive cells were detected within the optic nerves of all animal groups in contrast to a high amount of activated macrophages positive for ED1. This might be attributable the late time point analyzed in our study (day 21 of MOG-EAE). In

support of this notion, it has been shown in autoimmune diseases in humans that phagocytosis is inversely correlated with CD45 expression on polymorphonuclear cells.<sup>24</sup> Counting the numbers of CD3- and CD45-positive cells within the optic nerves, we found a significant decrease in the GA pretreatment group:  $16.9 \pm 2.6$  CD45-positive cells/mm<sup>2</sup> and  $1.3 \pm 0.5$  CD3-positive cells/mm<sup>2</sup> (mean ± SEM,  $P < 0.001$ ) after pretreatment in comparison to  $42.6 \pm 2$  CD45-positive cells/mm<sup>2</sup> and  $6 \pm 0.5$  CD3-positive cells/mm<sup>2</sup> in vehicle-treated animals (Figure 5, A, C, E–H). The extent of inflammation in the GA early ( $39.5 \pm 2.5$  CD45-positive cells/mm<sup>2</sup>,  $5.9 \pm 0.8$  CD3-positive cells/mm<sup>2</sup>) and late treatment groups ( $32.4 \pm 3.8$  CD45-positive cells/mm<sup>2</sup>,  $6.4 \pm 1.1$  CD3-positive cells/mm<sup>2</sup>) (Figure 5A) did not differ from the one of the vehicle-treated animals. As revealed by ED1 and H&E staining, the extent of inflammation after pretreatment was also significantly decreased in comparison to that in vehicle-treated animals (score of  $1.0 \pm 0.2$  versus  $2.2 \pm 0.3$  for ED1 staining; score of  $1.0 \pm 0.3$  versus  $2.3 \pm 0.3$  for H&E staining; mean ± SEM;  $P < 0.05$ ). Representative examples of ED1 and H&E stainings after GA pretreatment are given in Figure 5, I and K. The animals in the early and late treatment groups showed no differences in comparison to the control group ( $1.5 \pm 0.3$  for ED1 and  $2.1 \pm 0.4$  for H&E staining in the early GA

**Table 2.** Results of Visual Evoked Potentials (VEPs) and Electroretinograms (ERGs) Obtained on Days 1 and 8 of MOG-EAE (EAEd1 or EAEd8) in IFN-β-1b-Treated Animals and the Corresponding Control Group

	VEP EAEd1 flash	VEP EAEd8 flash	VEP EAEd1 pattern	VEP EAEd8 pattern	ERG EAEd1 flash	ERG EAEd8 flash	ERG EAEd1 pattern	ERG EAEd8 pattern
Pretreatment	5/8	4/8	0.18 ± 0.03 cyc/°	—	6/8	4/8	0.16 ± 0.02 cyc/°	—
Early therapy	4/8	2/8	—	—	5/8	3/8	—	—
Late therapy	4/8	1/8	—	—	5/8	2/8	—	—
Vehicle	5/8	2/8	—	—	7/8	3/8	—	—
Control: CFA- immunized (day 18 p.i.)	8/8		1.31 ± 0.16 cyc/°* (day 18 p.i.)		8/8 (day 18 p.i.)		1.10 ± 0.13 cyc/°* (day 18 p.i.)	

\*Statistically significant when compared with IFN-β-1b-treated animals ( $P < 0.005$ ). Control rats immunized with CFA were measured on day 18 after immunization (p.i.) as described previously.<sup>16</sup>

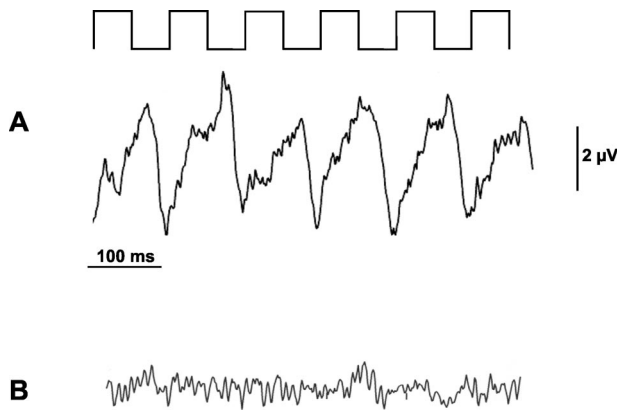


**Figure 2.** GA treatment started 14 days before immunization improves ERG responses during autoimmune optic neuritis. The stimulating pattern is indicated on top of the recording sequences. **A:** Example of ERG potentials at day 8 of MOG-EAE evoked by stimulation with six alternating bars in an animal treated with GA. **B:** Under the same recording conditions, only background noise levels of electrical activity were seen in an animal from the vehicle-treated group.

group;  $2.0 \pm 0.4$  for ED1 and  $2.6 \pm 0.2$  for H&E staining in the late GA group). In IFN- $\beta$ -1b-pretreated rats, the mean density of CD45- and CD3-positive cells was lower than the one of vehicle-treated controls, but this difference did not reach statistical significance ( $12.2 \pm 3.6$  CD45-positive cells/mm<sup>2</sup> and  $2.8 \pm 0.7$  CD3-positive cells/mm<sup>2</sup> versus  $31.6 \pm 8.3$  CD45-positive cells/mm<sup>2</sup> and  $4.9 \pm 0.5$  CD3-positive cells/mm<sup>2</sup> in the corresponding control group). In the early ( $28.3 \pm 6.1$  CD45-positive cells/mm<sup>2</sup>,  $4.5 \pm 0.6$  CD3-positive cells/mm<sup>2</sup>) and late treatment ( $24.7 \pm 5.3$  CD45-positive cells/mm<sup>2</sup>,  $4.2 \pm 0.9$  CD3-positive cells/mm<sup>2</sup>) groups of IFN- $\beta$ -1b, the extent of inflammation did not differ in comparison to vehicle-treated controls (Figure 5, B and D). As shown by ED1 and H&E staining, inflammatory infiltration in all three IFN- $\beta$ -1b-treated groups did not differ when compared with the vehicle-treated animals as well ( $1.7 \pm 0.2$  for ED1 and  $1.6 \pm 0.3$  for H&E staining in pretreated;  $1.6 \pm 0.2$  for ED1 and  $2.1 \pm 0.2$  for H&E staining in early;  $2.1 \pm 0.4$  for ED1 and  $2.5 \pm 0.4$  for H&E staining in late;  $2.0 \pm 0.3$  for ED1 and  $2.5 \pm 0.2$  for H&E staining of the corresponding vehicle-treated animals).

### Acute Axonal Damage of the Optic Nerve

Using APP as a marker for early axonal damage, we found the lowest number of APP-positive axons in the GA pretreatment group ( $7.8 \pm 2.3$  axons/mm<sup>2</sup>; vehicle:  $27.9 \pm 1.2$  axons/mm<sup>2</sup>; mean  $\pm$  SEM;  $P < 0.005$ ) (Figure 6, A, C, and D). In the GA early ( $24.2 \pm 2.4$  axons/mm<sup>2</sup>) and late treatment groups ( $19.7 \pm 2.2$  axons/mm<sup>2</sup>), the number of APP-positive axons did not differ from that of the vehicle-treated animals (Figure 6A). After IFN- $\beta$ -1b pretreatment, only a tendency toward a reduction of APP-positive axons was seen ( $14.1 \pm 4.2$  axons/mm<sup>2</sup> versus  $24.0 \pm 5.7$  for vehicle). In the IFN- $\beta$ -1b early treatment group, we found  $19.7 \pm 5.2$  APP-positive axons/mm<sup>2</sup>. After late treatment,  $13.3 \pm 3.8$  APP-positive axons/mm<sup>2</sup> were counted. These results did not significantly differ

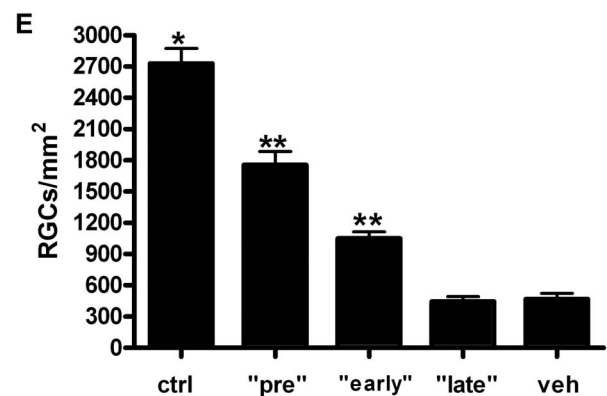
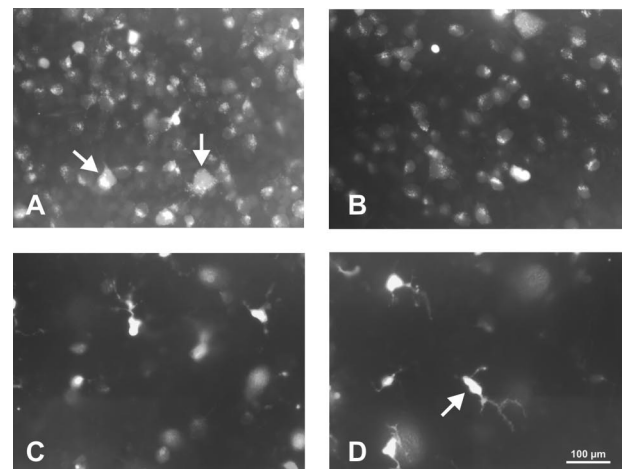


**Figure 3.** Pretreatment and early treatment with GA increases survival of RGCs during optic neuritis. Representative whole mount areas at 3/6 retinal radius from a GA pretreated (**A**), a GA early-treated (**B**), and GA late-treated (**C**) animal obtained at day 21 of MOG-EAE. **A:** Examples of FG-labeled RGCs are indicated by arrows. **D:** The number of FG-labeled RGCs in a corresponding vehicle-treated animal at day 21 of MOG-EAE is decreased when compared with GA treatment. Note the predominance of microglial cells in this retina (arrow). **E:** Data are given as the mean  $\pm$  SEM of retrogradely labeled RGCs/mm<sup>2</sup> at day 21 of MOG-EAE. ctrl, healthy sham-immunized control group; veh, vehicle treatment; pre, GA treatment started 14 days before immunization; early, GA treatment started at immunization; late, GA treatment started at the day of disease onset. \*Statistically significant when compared with all GA-treated rat groups ( $P < 0.005$  when compared with pretreatment;  $P < 0.0001$  when compared with early and late treatment). \*\*Statistically significant when compared with the vehicle-treated rat group ( $P < 0.0001$ ); one-way analysis of variance followed by Duncan's test). Scale bar = 100  $\mu$ m.

from those of the corresponding control group (Figure 6B). In all groups, the highest extent of APP-positive axons was found in actively demyelinating lesions.

### Chronic Axonal Damage and Demyelination of the Optic Nerve

In accordance with our electrophysiological findings, Bielschowsky silver impregnation revealed significantly higher axon counts at day 21 of MOG-EAE in the GA pretreatment group ( $4304 \pm 412.6$  axons/mm<sup>2</sup>; mean  $\pm$  SEM;  $P < 0.0001$ ) (Figure 7, C and I) when compared with vehicle-treated animals ( $644.3 \pm 90.8$  axons/mm<sup>2</sup>; Figure 7, C and J). In contrast, the axonal density of

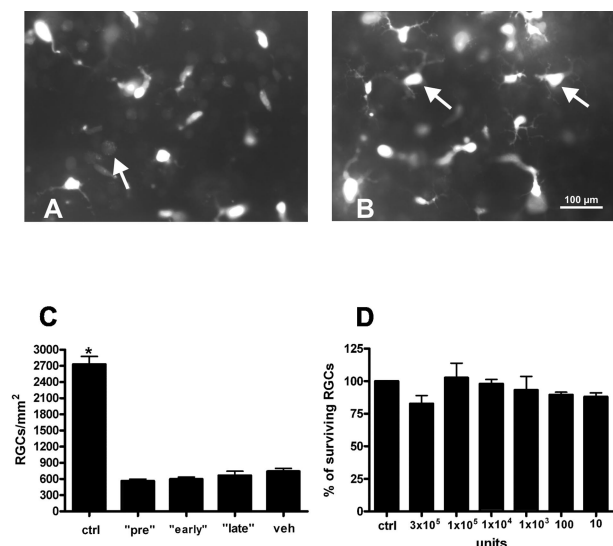


**Figure 4.** IFN-β-1b did not exert any rescue effect on RGCs. **A:** Representative whole mount area at 3/6 retinal radius from an IFN-β-1b-pretreated animal at day 21 of MOG-EAE. The **arrow** marks a remaining pale FG-positive RGC between microglial cells. **B:** Representative whole mount of a corresponding vehicle-treated animal. Microglial cells are indicated by **arrows**. **C:** Data are given as the mean ± SEM of retrogradely labeled RGCs/mm<sup>2</sup> at day 21 of MOG-EAE. ctrl, healthy sham-immunized control group; veh, vehicle treatment; pre, IFN-β-1b treatment started 14 days before immunization; early, IFN-β-1b treatment started at immunization; late, IFN-β-1b treatment started at the day of disease onset. \*Statistically significant when compared with all IFN-β-1b-treated rat groups ( $P < 0.0001$ ). **D:** IFN-β-1b has no direct influence on RGC survival *in vitro*. Indicated are the numbers of surviving immunopurified RGCs that were treated with different concentrations of IFN-β-1b (10×). Cell counts are expressed as a percentage of controls. Scale bar = 100 μm.

healthy, complete Freund's adjuvant-immunized animals was  $8680 \pm 1139$  axons/mm<sup>2</sup> (mean ± SEM,  $n = 8$ ). The extent of myelin damage determined as the percentage of the demyelinated area with respect to the whole optic nerve cross-section revealed a pronounced myelin preservation after pretreatment with GA ( $7.3 \pm 1.7\%$ , mean ± SEM,  $P < 0.0001$ ) (Figure 7, A and E) in comparison to the vehicle-treated controls ( $56.6 \pm 12.2\%$ ; Figure 7, A and F). Histopathological results in the group that received GA from the day of disease onset onwards did not differ from those of vehicle-treated rats. The number of remaining axons/mm<sup>2</sup> in the GA late treatment group was in the range of  $378.2 \pm 34.8$  (Figure 7C). The extent of demyelination was also similar to that of the vehicle-treated group: The mean percentage of the demyelinated area was  $74.0 \pm 11.8\%$  when GA treatment was initiated at disease onset. Axon counts and demyelination in the animals that received GA from the day of immunization onwards (early treatment) did not differ from the vehicle-treated control group as well ( $761.1 \pm 140.5$  axons/mm<sup>2</sup> and  $41.9 \pm 10.2\%$  demyelination versus  $644.3 \pm 90.8$  axons/mm<sup>2</sup> and  $56.6 \pm 12.2\%$  demyelination for vehicle) (Figure 7, A and C). The numbers of remaining axons that were present in IFN-β-1b-treated animals were in the range of  $525.1 \pm 107.8$  axons/mm<sup>2</sup> after pretreatment,  $377.3 \pm 81.9$  axons/mm<sup>2</sup> in the early treatment group, and  $320.3 \pm 70.5$  axons/mm<sup>2</sup> if therapy was started at disease onset. The mean axonal density in the corresponding control group ( $336.5 \pm 75.8$  axons/mm<sup>2</sup>) did

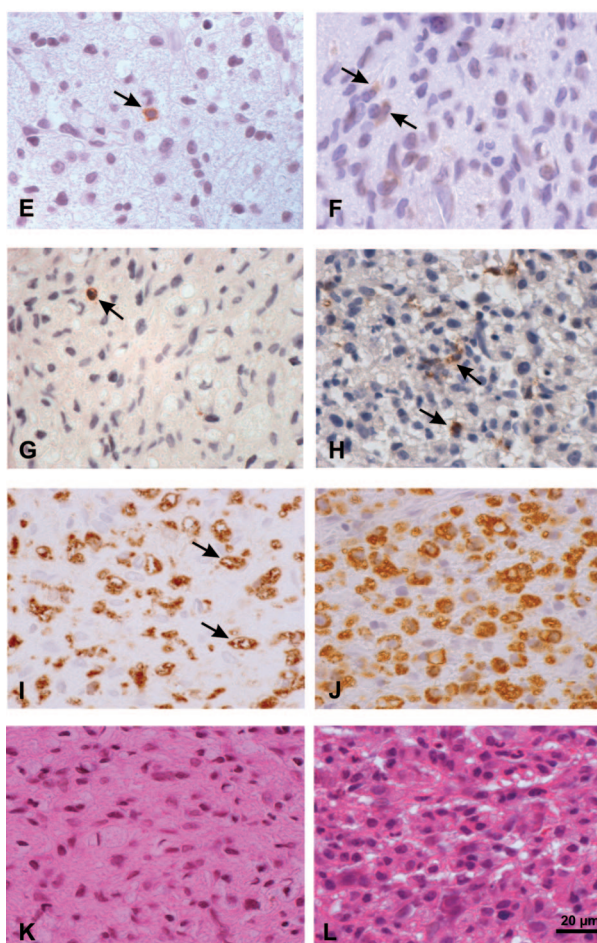
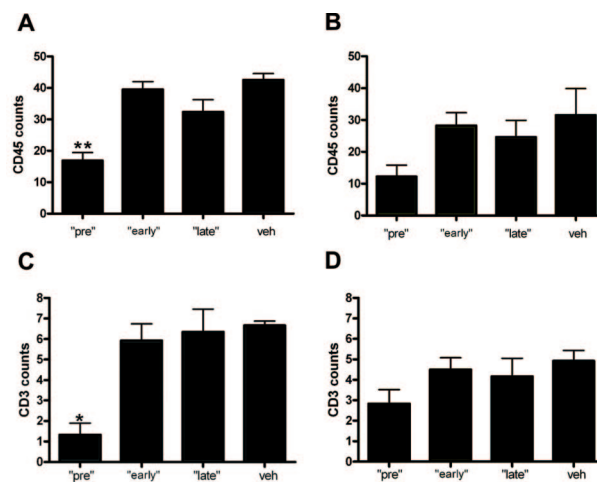


**Figure 5.** Decreased inflammatory infiltration of the optic nerves was found only in the rat group pretreated with GA. **A–D:** Data are given as the mean ± SEM of CD45-positive cells/mm<sup>2</sup> (**A, B**) or CD3-positive cells (**C, D**) at day 21 of MOG-EAE after treatment with GA (**A, C**) or IFN-β-1b (**B, D**). veh, vehicle treatment; pre, treatment with GA or IFN-β-1b started 14 days before immunization; early, GA or IFN-β-1b treatment started at immunization; late, GA or IFN-β-1b treatment started at the day of disease onset. Statistically significant when compared with the respective vehicle group (\* $P < 0.001$ ; \*\* $P < 0.0001$ ; one-way analysis of variance followed by Duncan's test). **E–H:** Representative optic nerve cross sections stained for CD45 (**E, F**) and CD3 (**G, H**) in a GA-pretreated animal (**E, G**) as well as in a vehicle-treated rat (**F, H**). CD45- and CD3-positive cells are indicated by **arrows**. **I–L:** Representative optic nerve cross-sections stained for ED1 (**I**) and H&E (**K**) in a GA-pretreated animal as well as a vehicle-treated rat (**J, L**). Examples of stained macrophages are indicated by **arrows**. Scale bar = 20 μm.



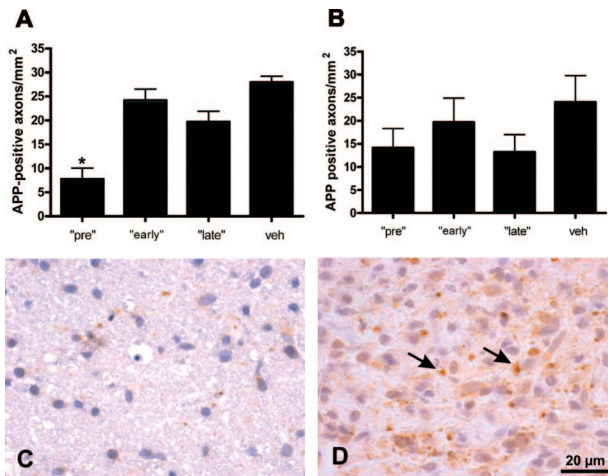


**Figure 6.** Only pretreatment with GA reduced acute axonal damage within the optic nerves. **A** and **B**: Data are given as the mean  $\pm$  SEM of APP-positive axons/mm<sup>2</sup> at day 21 of MOG-EAE after treatment with GA (**A**) or IFN- $\beta$ -1b (**B**). veh, vehicle treatment; pre, treatment with GA or IFN- $\beta$ -1b started 14 days before immunization; early, GA or IFN- $\beta$ -1b treatment started at immunization; late, GA or IFN- $\beta$ -1b treatment started at the day of disease onset. \*Statistically significant when compared with the vehicle group ( $P < 0.005$ ; one-way analysis of variance followed by Duncan's test). **C** and **D**: Representative optic nerve cross-sections stained for APP of a GA-pretreated animal (**C**) and a vehicle-treated rat (**D**). APP-positive axons are indicated by **arrows**. Scale bar = 20  $\mu$ m.

not significantly differ from any of the groups treated with IFN- $\beta$ -1b (Figure 7D). The mean percentage of the demyelinated area in all three groups treated with IFN- $\beta$ -1b was also similar to that of the vehicle-treated controls (vehicle:  $47.7 \pm 17.5\%$ ; pretreatment:  $55.7 \pm 10.3\%$ ; early treatment:  $49.7 \pm 11.3\%$ ; late treatment:  $32.5 \pm 8.7\%$ ; mean  $\pm$  SEM) (Figure 7B).

### Intracellular Signal Transduction in Retinal Ganglion Cells

The discrepancy between the histological data of the optic nerves, which showed a control-like extent of optic neuritis after early treatment with GA, and the increased RGC survival in that group suggests a primary neuroprotective effect of GA independent of its anti-inflammatory properties. Following this hypothesis, we investigated the influence of GA on retinal neurotrophic factor concentration as well as on several anti-apoptotic signaling steps in RGCs. Western blot analysis in our study revealed increased BDNF levels in retinal lysates of rats after treatment with GA (Figure 8B). In contrast, no changes in BDNF expression were detected after therapy with IFN- $\beta$ -1b (Figure 8C). Additionally, we investigated the retinal expression of BDNF during development and progression of naïve EAE (day 7 after immunization as well as on days 1, 8, and 21 of the disease). Whereas the amount of BDNF was comparable at the days of manifest EAE, a tendency toward a decreased protein expression was observed at day 7 after immunization (Figure 8A).

To investigate further the involved neurotrophin-dependent intracellular signal transduction in the GA-treated group of animals, we analyzed the phosphorylation of MAPKs and Akt as well as the expression of two

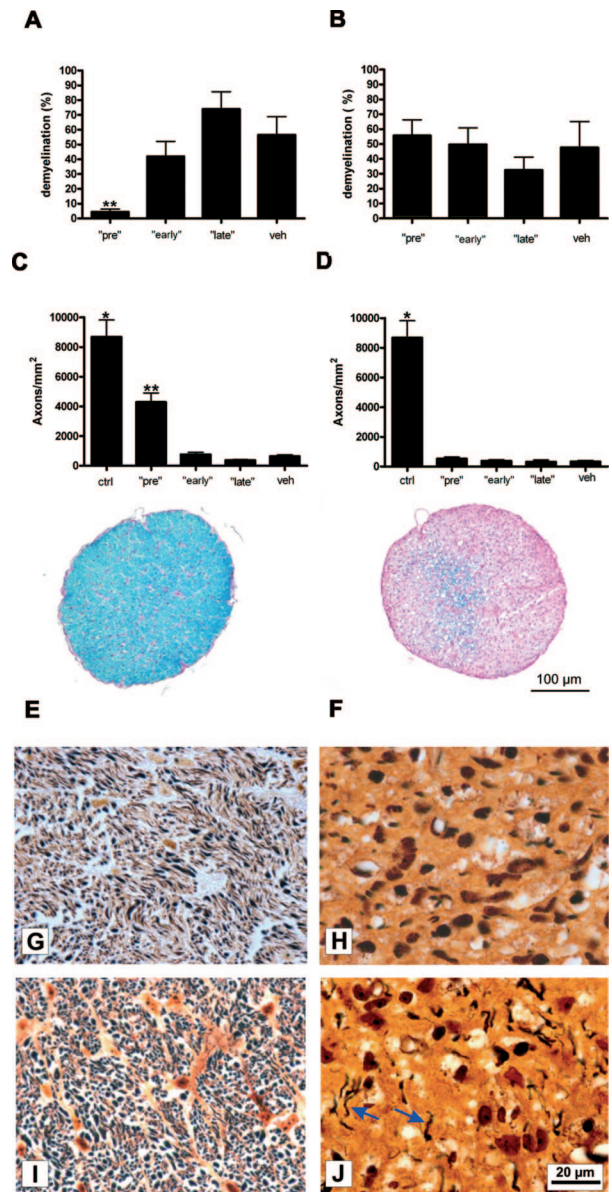


**Figure 7.** Decreased extent of demyelination and chronic axonal damage within the optic nerves of GA pretreated rats. **A** and **B**: Data are given as the mean percentage of the demyelinated area with respect to the whole optic nerve cross-section after GA (**A**) or IFN- $\beta$ -1b (**B**) treatment. **C** and **D**: Data are given as the mean  $\pm$  SEM of axons/mm<sup>2</sup> after application of GA (**C**) or IFN- $\beta$ -1b (**D**). ctrl, healthy sham-immunized control group; veh, vehicle treatment; pre, treatment with GA or IFN- $\beta$ -1b started 14 days before immunization; early, GA or IFN- $\beta$ -1b treatment started at immunization; late, GA or IFN- $\beta$ -1b treatment started at the day of disease onset. \*Statistically significant when compared with all GA- or IFN- $\beta$ -1b-treated animal groups ( $P < 0.0001$ ) \*\*Statistically significant when compared with vehicle-treated rats ( $P < 0.0001$ ; one-way analysis of variance followed by Duncan's test). **E** and **F**: Representative transverse optic nerve cross-sections stained with Luxol fast blue obtained from a GA-pretreated (**E**) and a vehicle-treated rat (**F**). **E**: Pronounced myelin preservation (blue) was detected after GA pretreatment. **F**: The optic nerve after application of vehicle appears extensively demyelinated (purple). **G** and **H**: Bielschowsky silver impregnation of an optic nerve from a healthy, sham-immunized rat (**G**) and an IFN- $\beta$ -1b-treated animal (**H**). **I** and **J**: Marked axonal preservation within the optic nerve of a GA-pretreated rat (**I**) when compared with the one of a vehicle-treated animal (**J**). **Blue arrows** indicate remaining axons. Scale bars: 100  $\mu$ m (**E**, **F**); 20  $\mu$ m (**G**-**J**).

members of the Bcl-2 family, Bcl-2 and Bax. The respective immunoblotting results are shown in Figure 8B: GA increased the phosphorylation of MAPKs when com-

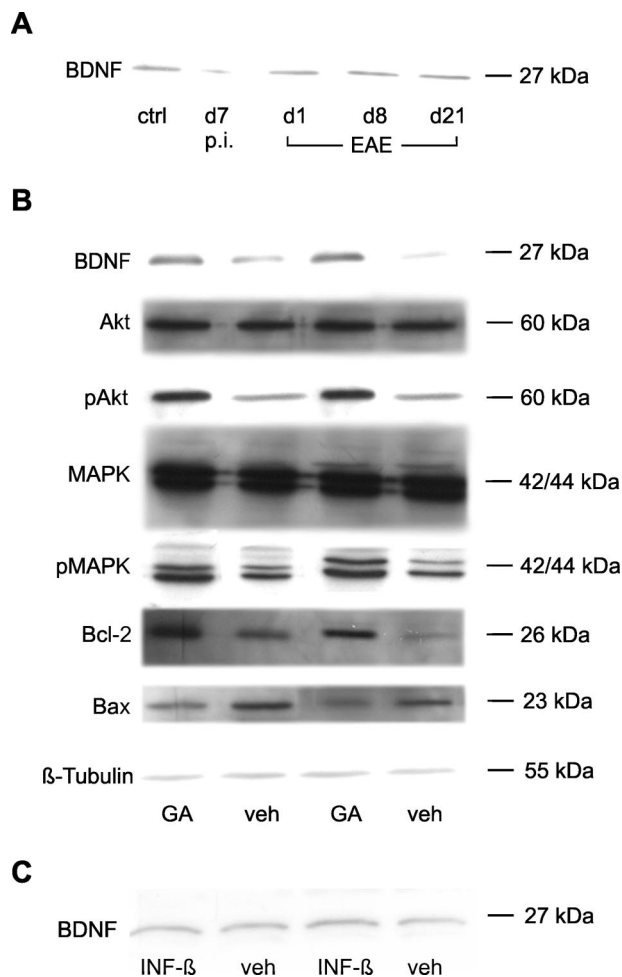


**Figure 8. A:** Western blot analysis of BDNF expression during development and progression of naïve MOG-EAE. The amount of BDNF slightly decreased at day 7 after immunization. Ctrl, healthy sham-immunized control; d7 p.i., day 7 after immunization; d1 EAE, day 1 of EAE; d8 EAE, day 8 of EAE; d21 EAE, day 21 of EAE. **B:** GA increases retinal BDNF concentration and activates protective intracellular signaling cascades in RGCs. In each column, Western blot analyses of different proteins using the same retinal protein lysate are shown. Note the increase of retinal BDNF levels under GA treatment. GA also induces the phosphorylation of Akt (pAkt) and MAPKs (pMAPK). The unphosphorylated forms of these proteins are similar in each group. Bcl-2 levels are increased under GA therapy whereas the expression of Bax is decreased. Expression levels of  $\beta$ -tubulin as a housekeeping protein were similar in the different probes analyzed. **C:** No differences in BDNF expression levels were found with INF- $\beta$  treatment when compared with vehicle-treated animals.

pared with the injection of NaCl. In contrast, the unphosphorylated inactive form of these proteins was not influenced by GA treatment. GA also increased the phosphorylation of Akt when compared with vehicle-treated animals. Furthermore, GA treatment induced an up-regulation of the anti-apoptotic protein Bcl-2 and simultaneously decreased the expression of the proapoptotic protein Bax (Figure 8B).

### Discussion

Axonal damage has the strongest impact on the development of irreversible neurological symptoms in MS.<sup>1,25–27</sup> Data that allow an estimation of the effects of

immunomodulatory therapies on neurodegeneration in this disease come from magnetic resonance imaging and magnetic resonance spectroscopy studies. However, the results of these studies are contradictory.<sup>5–8,28–32</sup>

In addition to severe axonal pathology, histopathological studies demonstrated apoptotic neuronal cell death in demyelinated cerebral cortex lesions of MS patients,<sup>2</sup> which cannot be assessed by imaging techniques. As known from studies of classical neurodegenerative diseases such as Parkinson's and Alzheimer's disease, it is difficult to detect apoptotic neurons in human brain tissue because of the rapid time kinetics of apoptosis-related intracellular signaling cascades.<sup>33</sup> For this reason, much of the present knowledge about apoptotic neuronal cell death and its mechanisms in MS comes from studies in EAE models. MOG-induced optic neuritis, the model used in our present study, is suitable for testing neuroprotective agents because it leads to acute apoptotic cell death of RGCs, the neurons that form the axons of the optic nerve.<sup>16</sup> Recently, we described the kinetics of RGC apoptosis in this model starting  $\sim$ 1 week before manifestation of clinical signs and rapidly progressing until day 8 of the disease.<sup>17</sup> Under autoimmune inflammatory conditions, a close association between neurodegeneration and inflammation has been demonstrated.<sup>1</sup> This led to the concept that protection of neurons might be achieved secondary to an anti-inflammatory or immunomodulatory treatment. To determine whether, and by which mechanisms, IFN- $\beta$ 1b and GA protect RGCs from apoptosis during MOG-induced optic neuritis, we investigated the survival and function of these neurons. As revealed by VEP and ERG recordings, GA improved visual functions in the animals if treatment was started 14 days before immunization or, with lesser effect, if GA was given from the day of immunization onwards. IFN- $\beta$ 1b, in contrast, did not have any influence on visual functions of rats during MOG-EAE. In accordance with the electrophysiological data, the survival of RGCs in these two GA-treated rat groups was promoted. Whereas GA pretreatment decreased the severity of optic neuritis, histopathological results of the optic nerves did not differ from those of the vehicle-treated controls if therapy with GA was started at immunization. The observation of an increased RGC survival but unchanged optic nerve damage in this group suggests an additional inflammation-independent protective effect of GA on RGCs. Evidence for GA-induced neuroprotection under noninflammatory conditions came from studies in nerve injury models.<sup>34–36</sup> In EAE, it was reported that axonal damage in mice was reduced after GA therapy.<sup>37</sup> However, axon protection in this study seemed to be the consequence of the anti-inflammatory/immunomodulatory properties of the agent.

As known from studies with immunosuppressive therapies, elimination of the inflammatory component of MS does not necessarily stop neurodegeneration.<sup>38,39</sup> In the context of neuroprotective immunity, it has been described that immune cells supply several neuroprotective mediators such as nerve growth factor or glial cell line-derived neurotrophic factor.<sup>40–42</sup> GA-specific human T-cell lines are known to produce neurotrophins including BDNF.<sup>10</sup> Neurotrophic factors in turn activate a variety of

protective intracellular neuronal pathways.<sup>43,44</sup> In our present study, we show that GA induced the phosphorylation of MAPKs and Akt in RGCs via increasing retinal concentrations of BDNF. Furthermore, treatment with GA led to a shift in the Bcl-2 family of proteins toward the anti-apoptotic side. Similar effects on RGC signal transduction in our model have been observed under therapies with neuroprotective agents such as Epo<sup>45</sup> or CNTF.<sup>46</sup> In contrast, we have demonstrated that anti-inflammatory treatment with methylprednisolone increased apoptosis of RGCs during optic neuritis by inhibition of MAPK phosphorylation although inflammatory infiltration of the optic nerve was reduced.<sup>23</sup> This proapoptotic effect of the steroid could be antagonized by simultaneous treatment with the neurotrophic factor Epo.<sup>18</sup> Based on these data, increased secretion of neurotrophic factors and activation of neurotrophin-dependent signaling pathways by GA might help to compensate for the lack of endogenous neurotrophin production resulting from anti-inflammatory treatment. To support this hypothesis, decreased levels of BDNF have been found in patients with RR-MS, which was reversed by therapy with GA.<sup>47</sup>

In summary, we present evidence for positive influences of early IFN- $\beta$  or GA treatment on disease activity in a rat model of MOG-EAE. Measuring neurodegeneration and neuronal function in this model revealed that only treatment with GA exerted protective effects on RGCs. It is apparent that both IFN- $\beta$ -1b and GA are potent drugs that act on different aspects of MS-associated pathophysiology. Considering the clinical and histopathological heterogeneity of MS,<sup>48</sup> successful future therapies should be more individually adjusted. As a precondition for such individual therapeutic concepts, clinical markers must be established to allow identification of those patients endangered by early neurodegeneration.

### Acknowledgments

We thank Doron Merkler and Christine Stadelmann for providing myelin oligodendrocyte glycoprotein and Inna Boger and Nadine Meyer for expert technical assistance.

### References

1. Trapp BD, Peterson J, Ransohoff RM, Rudick R, Mork S, Bo L: Axonal transection in the lesions of multiple sclerosis. *N Engl J Med* 1998, 338:278–285
2. Peterson JW, Bo L, Mork S, Chang A, Trapp BD: Transected neurites, apoptotic neurons, and reduced inflammation in cortical multiple sclerosis lesions. *Ann Neurol* 2001, 50:389–400
3. Paty DW, Li DK: Interferon  $\beta$ -1b is effective in relapsing-remitting multiple sclerosis. II. MRI analysis results of a multicenter, randomized, double-blind, placebo-controlled trial UBC MS/MRI Study Group and the IFNB Multiple Sclerosis Study Group. *Neurology* 1993, 43:662–667
4. Sela M, Teitelbaum D: Glatiramer acetate in the treatment of multiple sclerosis. *Expert Opin Pharmacother* 2001, 2:1149–1165
5. Comi G, Filippi M, Barkhof F, Durelli L, Edan G, Fernandez O, Hartung H, Seeldrayers P, Sorensen PS, Rovaris M, Martinelli V, Hommes OR, Early Treatment of Multiple Sclerosis Study Group: Effect of early

- interferon treatment on conversion to definite multiple sclerosis: a randomised study. *Lancet* 2001, 357:1576–1582
6. Rovaris M, Filippi M: Interventions for the prevention of brain atrophy in multiple sclerosis: current status. *CNS Drugs* 2003, 17:563–575
7. Narayanan S, De Stefano N, Francis GS, Arnaoutelis R, Caramanos Z, Collins DL, Pelletier D, Arnason BGW, Antel JP, Arnold DL: Axonal metabolic recovery in multiple sclerosis patients treated with interferon  $\beta$ -1b. *J Neurol* 2001, 248:979–986
8. Parry A, Corkill R, Blamire AM, Palace J, Narayanan S, Arnold D, Styles P, Matthews PM: Beta-interferon treatment does not always slow the progression of axonal injury in multiple sclerosis. *J Neurol* 2003, 250:171–178
9. Yong VW: Differential mechanisms of action of interferon- $\beta$  and glatiramer acetate in MS. *Neurology* 2002, 59:802–808
10. Ziemssen T, Kumpfel T, Schneider H, Klinkert WE, Neuhaus O, Hohlfeld R: Secretion of brain-derived neurotrophic factor by glatiramer acetate-reactive T-helper cell lines: implications for multiple sclerosis therapy. *J Neurol Sci* 2005, 233:109–112
11. Biernacki K, Antel JP, Blain M, Narayanan S, Arnold DL, Prat A: Interferon  $\beta$  promotes nerve growth factor secretion early in the course of multiple sclerosis. *Arch Neurol* 2005, 62:563–568
12. Adelman M, Wood J, Benzel I, Fiori P, Lassmann H, Matthieu JM, Gardinier MV, Dornmair K, Linington C: The N-terminal domain of the myelin oligodendrocyte glycoprotein (MOG) induces acute demyelinating experimental autoimmune encephalomyelitis in the Lewis rat. *J Neuroimmunol* 1995, 63:17–27
13. Johns TG, Kerlero de Rosbo N, Menon KK, Abo S, Gonzales MF, Bernard CC: Myelin oligodendrocyte glycoprotein induces a demyelinating encephalomyelitis resembling multiple sclerosis. *J Immunol* 1995, 154:5536–5541
14. Storch MK, Stefferl A, Brehm U, Weissert R, Wallstrom E, Kerschensteiner M, Olsson T, Linington C, Lassmann H: Autoimmunity to myelin oligodendrocyte glycoprotein in rats mimics the spectrum of multiple sclerosis pathology. *Brain Pathol* 1998, 8:681–694
15. Weissert R, Wallstrom E, Storch MK, Stefferl A, Lorentzen J, Lassmann H, Linington C, Olsson T: MHC haplotype-dependent regulation of MOG-induced EAE in rats. *J Clin Invest* 1998, 102:1265–1273
16. Meyer R, Weissert R, Diem R, Storch MK, de Graaf KL, Kramer B, Bähr M: Acute neuronal apoptosis in a rat model of multiple sclerosis. *J Neurosci* 2001, 21:6214–6220
17. Hobom M, Storch MK, Weissert R, Maier K, Radhakrishnan A, Kramer B, Bähr M, Diem R: Mechanisms and time course of neuronal degeneration in experimental autoimmune encephalomyelitis. *Brain Pathol* 2004, 14:148–157
18. Diem R, Sättler MB, Merkler D, Demmer I, Maier K, Stadelmann C, Ehrenreich H, Bähr M: Combined therapy with methylprednisolone and erythropoietin in a model of multiple sclerosis. *Brain* 2005, 128:375–385
19. van der Meide PH, de Labie MC, Ruuls SR, Groenestein RJ, Botman CA, Olsson T, Dijkstra CD: Discontinuation of treatment with IFN- $\beta$  leads to exacerbation of experimental autoimmune encephalomyelitis in Lewis rats. Rapid reversal of the antiproliferative activity of IFN- $\beta$  and excessive expansion of autoreactive T cells as disease promoting mechanisms. *J Neuroimmunol* 1998, 84:14–23
20. Barres BA, Silverstein BE, Corey DP, Chun LL: Immunological, morphological, and electrophysiological variation among retinal ganglion cells purified by panning. *Neuron* 1988, 1:791–803
21. Mosmann T: Rapid colorimetric assay for cellular growth and survival: application to proliferation and cytotoxicity assays. *J Immunol Methods* 1983, 65:55–63
22. Diem R, Meyer R, Weishaupt JH, Bähr M: Reduction of potassium currents and phosphatidylinositol 3-kinase-dependent AKT phosphorylation by tumor necrosis factor-( $\alpha$ ) rescues axotomized retinal ganglion cells from retrograde cell death in vivo. *J Neurosci* 2001, 21:2058–2066
23. Diem R, Hobom M, Maier K, Weissert R, Storch MK, Meyer R, Bähr M: Methylprednisolone increases neuronal apoptosis during autoimmune CNS inflammation by inhibition of an endogenous neuroprotective pathway. *J Neurosci* 2003, 23:6993–7000
24. Bohm I: Environment-dependent down-modulation of CD45 cell surface expression on polymorphonuclear cells. *J Clin Lab Anal* 2004, 18:187–194
25. Ferguson B, Matyszak MK, Esiri MM, Perry VH: Axonal damage in acute multiple sclerosis lesions. *Brain* 1997, 120:393–399

26. Kornek B, Storch MK, Weissert R, Wallstroem E, Steffler A, Olsson T, Linington C, Schmidbauer M, Lassmann H: Multiple sclerosis and chronic autoimmune encephalomyelitis: a comparative quantitative study of axonal injury in active, inactive, and remyelinated lesions. *Am J Pathol* 2000, 157:267–276
27. Filippi M, Rocca MA, Comi G: The use of quantitative magnetic-resonance-based techniques to monitor the evolution of multiple sclerosis. *Lancet Neurol* 2003, 2:337–346
28. Arnold DL: Magnetic resonance spectroscopy: imaging axonal damage in MS. *J Neuroimmunol* 1999, 98:2–6
29. Brex PA, Molyneux PD, Smiddy P, Barkhof F, Filippi M, Yousry TA, Hahn D, Rolland Y, Salonen O, Pozzilli C, Polman CH, Thompson AJ, Kappos L, Miller DH: The effect of IFN $\beta$ -1b on the evolution of enhancing lesions in secondary progressive MS. *Neurology* 2001, 57:2185–2190
30. Paty DW, Li DK: Interferon  $\beta$ -1b is effective in relapsing-remitting multiple sclerosis. II MRI analysis results of a multicenter, randomized, double-blind, placebo-controlled trial. 1993. *Neurology* 2001, 57:S10–S15
31. Ge Y, Grossman RI, Udupa JK, Fulton J, Constantinescu CS, Gonzales-Scarano F, Babb JS, Mannon LJ, Kolson DL, Cohen JA: Glatiramer acetate (Copaxone) treatment in relapsing-remitting MS: quantitative MR assessment. *Neurology* 2000, 54:813–817
32. Khan O, Shen Y, Cao C, Bao F, Ching W, Reznar M, Buccheister A, Hu J, Latif Z, Tselis A, Lisak AR: Axonal metabolic recovery and potential neuroprotective effect of glatiramer acetate in relapsing-remitting multiple sclerosis. *Multiple Sclerosis* 2005, 11:1–6
33. Mattson MP: Apoptosis in neurodegenerative disorders. *Nat Rev Mol Cell Biol* 2000, 1:120–129
34. Kipnis J, Yoles E, Porat Z, Cohen A, Mor F, Sela M, Cohen IR, Schwartz M: T cell immunity to copolymer 1 confers neuroprotection on the damaged optic nerve: possible therapy for optic neuropathies. *Proc Natl Acad Sci USA* 2000, 97:7446–7451
35. Angelov DN, Waibel S, Guntinas-Lichius O, Lenzen M, Neiss WF, Tomov TL, Yoles E, Kipnis J, Schori H, Reuter A, Ludolph A, Schwartz M: Therapeutic vaccine for acute and chronic motor neuron diseases: implications for amyotrophic lateral sclerosis. *Proc Natl Acad Sci USA* 2003, 100:4790–4795
36. Schori H, Kipnis J, Yoles E, WoldeMussie E, Ruiz G, Wheeler LA, Schwartz M: Vaccination for protection of retinal ganglion cells against death from glutamate cytotoxicity and ocular hypertension: implications for glaucoma. *Proc Natl Acad Sci USA* 2001, 98:3398–3403
37. Gilgun-Sherki Y, Panet H, Holdengreber V, Mosberg-Galili R, Offen D: Axonal damage is reduced following glatiramer acetate treatment in C57/bl mice with chronic-induced experimental autoimmune encephalomyelitis. *Neurosci Res* 2003, 47:201–207
38. Rice GP, Filippi M, Comi G: Cladribine and progressive MS: clinical and MRI outcomes of a multicenter controlled trial. Cladribine MRI Study Group. *Neurology* 2000, 54:1145–1155
39. Paolillo A, Coles AJ, Molyneux PD, Gawne-Cain M, MacManus D, Barker GJ, Compston DA, Miller DH: Quantitative MRI in patients with secondary progressive MS treated with monoclonal antibody Campath 1H. *Neurology* 1999, 53:751–757
40. Kerschensteiner M, Gallmeier E, Behrens L, Leal VV, Misgeld T, Klinkert WE, Kolbeck R, Hoppe E, Oropeza-Wekerle RL, Bartke I, Stadelmann C, Lassmann H, Wekerle H, Hohlfeld R: Activated human T cells, B cells, and monocytes produce brain-derived neurotrophic factor in vitro and in inflammatory brain lesions: a neuroprotective role of inflammation? *J Exp Med* 1999, 189:865–870
41. Batchelor PE, Liberatore GT, Wong JY, Porritt MJ, Frerichs F, Donnan GA, Howells DW: Activated macrophages and microglia induce dopaminergic sprouting in the injured striatum and express brain-derived neurotrophic factor and glial cell line-derived neurotrophic factor. *J Neurosci* 1999, 19:1708–1716
42. Hammarberg H, Lidman O, Lundberg C, Eltayeb SY, Gielen AW, Muhallab S, Svenningsson A, Linda H, van Der Meide PH, Cullheim S, Olsson T, Piehl F: Neuroprotection by encephalomyelitis: rescue of mechanically injured neurons and neurotrophin production by CNS-infiltrating T and natural killer cells. *J Neurosci* 2000, 20:5283–5291
43. Yamada M, Tanabe K, Wada K, Shimoke K, Ishikawa Y, Ikeuchi T, Koizumi S, Hatanaka H: Differences in survival-promoting effects and intracellular signaling properties of BDNF and IGF-1 in cultured cerebral cortical neurons. *J Neurochem* 2001, 78:940–951
44. Barnabe-Heider F, Miller FD: Endogenously produced neurotrophins regulate survival and differentiation of cortical progenitors via distinct signaling pathways. *J Neurosci* 2003, 23:5149–5160
45. Sättler MB, Merkler D, Maier K, Stadelmann C, Ehrenreich H, Bähr M, Diem R: Neuroprotective effects and intracellular signaling pathways of erythropoietin in a rat model of multiple sclerosis. *Cell Death Differ* 2004, 11(Suppl 2):S181–S192
46. Maier K, Rau CR, Storch MK, Sättler MB, Demmer I, Weissert R, Taheri N, Kuhnert AV, Bähr M, Diem R: Ciliary neurotrophic factor protects retinal ganglion cells from secondary cell death during acute autoimmune optic neuritis in rats. *Brain Pathol* 2004, 14:378–387
47. Azoulay D, Vachapova V, Shihman B, Miler A, Karni A: Lower brain-derived neurotrophic factor in serum of relapsing remitting MS: reversal by glatiramer acetate. *J Neuroimmunol* 2005, 167:215–218
48. Lassmann H, Brück W, Lucchinetti C: Heterogeneity of multiple sclerosis pathogenesis: implications for diagnosis and therapy. *Trends Mol Med* 2001, 7:115–121